Computers and Concrete, *Vol. 21, No. 3 (2018) 231-237*
DOI: https://doi.org/10.12989/cac.2018.21.3.231

Tensile strain-hardening behaviors and crack patterns of slag-based fiber-reinforced composites

Seung-Jun Kwon[1a], Jeong-Il Choi[2b], Huy Hoàng Nguyễn[2b] and Bang Yeon Lee[*2]

[1]*Department of Civil Engineering, Hannam University, Daejeon 34430, Republic of Korea*
[2]*School of Architecture, Chonnam National University, Gwangju 61186, Republic of Korea*

(Received May 1, 2017, Revised September 12, 2017, Accepted October 27, 2017)

Abstract. A strain-hardening highly ductile composite based on an alkali-activated slag binder and synthetic fibers is a promising construction material due to its excellent tensile behavior and owing to the ecofriendly characteristics of its binder. This study investigated the effect of different types of synthetic fibers and water-to-binder ratios on the compressive strength and tensile behavior of slag-based cementless composites. Alkali-activated slag was used as a binder and water-to-binder ratios of 0.35, 0.45, and 0.55 were considered. Three types of fibers, polypropylene fiber, polyethylene (PE) fiber, and polyparaphenylene -benzobisethiazole (PBO) fiber, were used as reinforcing fibers, and compression and uniaxial tension tests were performed. The test results showed that the PE fiber series composites exhibited superior tensile behavior in terms of the tensile strain capacity and crack patterns while PBO fiber series composites had high tensile strength levels and tight crack widths and spacing distances.

Keywords: alkali-activator; cementless composite; compressive strength; slag; synthetic fiber; tensile behavior

1. Introduction

The performance of a fiber-reinforced cementitious composite is determined by the fiber bridging behavior, which is influenced by the properties of the fiber, the matrix, and the interface between the fiber and the matrix at a cracked plane (Kanda and Li 1998, Yang *et al*. 2008, Lee *et al*. 2010, Lee *et al*. 2010, Huang and Huang 2011). Therefore, to achieve high ductility in a fiber-reinforced cementitious composite through multiple instances of micro-cracking, the type of matrix and the mixture proportion, as well as the type of fiber, are important. Among synthetic fibers, polyethylene (PE), polyvinyl-alcohol (PVA), and polypropylene (PP) have been successfully adopted for high ductility in fiber-reinforced cementitious composites (Maalej and Li 1994, Li *et al*. 2001, Li 2012, Ranade *et al*. 2013, Li *et al*. 2014, Cho *et al*. 2015, Felekoglu and Keskinates 2016, Kang *et al*. 2016, Tosun-Felekoğlu *et al*. 2017). Recently, researchers have attempted to achieve high ductility and what can be termed as 'material greenness' by developing fiber-reinforced cementless composites using cementless binders such as alkali-activated slag and geopolymer and PE and PVA fibers (Lee *et al*. 2012, Ohno and Li 2014, Choi *et al*. 2015, Nematollahi *et al*. 2015, Nematollahi *et al*. 2015, Choi *et al*. 2016, Choi *et al*. 2016). Lee *et al.* (2012) developed a fiber-reinforced cementless composite with a compressive strength of 30.6 MPa, a tensile strength of 4.7 MPa, and a tensile strain capacity of 4.5 % using alkali-activated slag-based mortar and PVA fibers (Lee *et al*. 2012). Ohno and Li (2014) developed another type of fiber-reinforced cementless composite with a compressive strength of 27.6 MPa, a tensile strength of 3.4 MPa, and a tensile strain capacity of 4.3 % using fly ash-based geopolymer mortar and PVA fibers (Ohno and Li 2014). Nematollahi *et al.* (2015) also developed a geopolymer based on fly ash with higher compressive strength up to 63.7 MPa and a tensile strain capacity up to 4.3 % (Nematollahi *et al*. 2015). More recently, Choi *et al*. (2016) reported a composite using alkali-activated slag and high strength PE fiber with a compressive strength of 54.8 MPa and extremely high tensile strain capacity up to 7.5%. The toughness of composite was 2.7 times higher than that of PE-ECC (engineered cementitious composites) and 1.8 times higher than that of high-strength and high-ductility concrete. (Maalej and Li 1994, Ranade *et al*. 2013, Choi *et al*. 2016).

It has been demonstrated that a cementless alkali-activated composite reinforced with PVA and PE fibers has high tensile strain capacity. However, to the best of the authors' knowledge, the literature on the composite properties of cementless alkali-activated composites reinforced by other types of fibers, such as PP fiber and polyparaphenylene-benzobisethiazole (PBO) fiber, remains limited. PP fiber has a low chemical bond between the fiber and the matrix and relatively low tensile strength compared to those of PVA and PE fibers (Felekoglu *et al*. 2014). On the other hand, PBO fiber has high tensile strength up to 5,800 MPa. Therefore, it can be expected that PBO fiber-reinforced composite has high fiber bridging capacity at the crack plane. The purpose of this study was to investigate experimentally the tensile strain-hardening behaviors and

∗Corresponding author, Associate Professor
E-mail: bylee@jnu.ac.kr
[a]Ph.D.
[b]Graduate Student

ISSN: 1598-8198 (Print), 1598-818X (Online)

Table 1 Chemical composition of the GGBFS

CaO	SiO_2	Al_2O_3	MgO	SO_3	TiO_2	Fe_2O_3	K_2O	etc.
44.6	31.5	13	4.9	3.4	0.8	0.5	0.5	0.9

Table 2 Properties of fibers

Type of fiber	Diameter (μm)	Length (mm)	Tensile strength (MPa)	Density (g/cm^3)	Elastic modulus (GPa)
PP	12	10	850	0.91	6
PE	16	12	3,030	0.97	112
PBO	12	12	5,800	1.54	180

Table 3 Mixture proportions (weight ratio)

Mixtures	Binder	Water	SP	VMA	Fiber type
PP-0.35	1	0.35	0.0010	0.0001	PP
PP-0.45	1	0.45	0.0002	0.0003	PP
PP-0.55	1	0.55	-	0.0013	PP
PE-0.35	1	0.35	0.0010	0.0001	PE
PE-0.45	1	0.45	0.0002	0.0004	PE
PE-0.55	1	0.55	-	0.0017	PE
PBO-0.35	1	0.35	0.0014	0.0010	PBO
PBO-0.45	1	0.45	0.0010	0.0010	PBO
PBO-0.55	1	0.55	-	0.0022	PBO

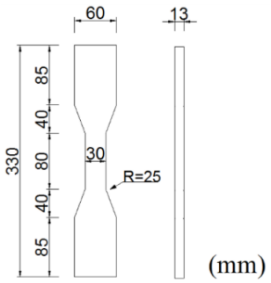

(a)

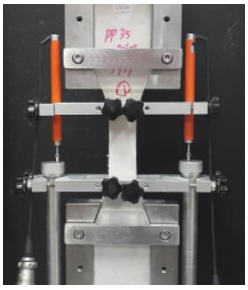

(b)

Fig. 1 Uniaxial tension test: (a) specimen geometry; (b) test setup

crack patterns of alkali-activated slag-based cementless composites reinforced with synthetic fibers and the effect of different types of synthetic fibers on the compressive strength and tensile behavior of the composites with the identical water-to-binder ratios.

2. Materials and methods

2.1 Materials and mixture proportion

Alkali-activated slag was used as a binder. Ground-granulated blast furnace slag (GGBFS) was used as a source material, and two types of alkali-activators, calcium hydroxide and sodium sulfate, were used in powder form to prevent quick setting. The weight ratios of calcium hydroxide and sodium sulfate were 8.38 % and 3.35 % of GGBFS, respectively. The fineness value and specific gravity of the slag were 4,320 cm^2/g and 2.92, respectively. The chemical composition of the GGBFS is listed in Table 1.

In order to investigate the effect of the water-to-binder ratio, three ratios were used: 0.35, 0.45, and 0.55. Li and Li experimentally investigated the effect of the plastic viscosity of the matrix on the tensile strain capacity and fiber dispersion (Li and Li 2013). They found that the fiber dispersion was poor and therefore induced a low tensile strain capacity when the plastic viscosity of the matrix fell below 5.0 Pa.s. In order to achieve a good fiber dispersion, the optimized amounts of the superplasticizer (SP) and viscosity-modifying admixture (VMA) were included for each mixture. The PP, PE, and PBO fibers were used as reinforcing fibers. The properties of the three types of fibers are given in Table 2. Table 3 lists the mixture proportions investigated in this study, and all mixtures had the same volume of fibers (1.75% of the total volume).

2.2 Specimen preparation

Each composition was mixed in a planetary mixer. The GGBFS and alkali-activators were mixed for three minutes. Subsequently, water, SP, and VMA were added and mixed for another five minutes. After achieving a proper plastic viscosity of the mixture, fibers were slowly added to the mixer and then mixed for five minutes. Afterwards, the mixture was cast into molds for compressive strength and uniaxial tension tests. For each mixture, three 50 mm cube specimens were prepared for the compressive strength test, with six dog-bone shape specimens (Fig. 1(a)) created for the tension test. A plastic sheet was used to cover the molds to prevent the evaporation of surface water from the mixture, and all of the mixtures were cured in a control room at a (23±3)℃ for two days. The hardened mixtures were removed from the molds and cured in water at a temperature of (23±3)℃ until an age of 28 days.

2.3 Compression and uniaxial tension tests

The compressive strength test was conducted according to ASTM C109-07 (ASTM 2007). The tensile behavior, quantitatively expressed by the first-cracking strength, tensile strength, and tensile strain capacity, of each mixture was investigated with uniaxial tension tests. The dimensions of the specimen for the uniaxial tension tests and the test method were in accordance with Japan Society of Civil Engineers recommendations as no standard with regard to the uniaxial tension tests is available (JSCE 2008). The tensile load by displacement control was applied to a

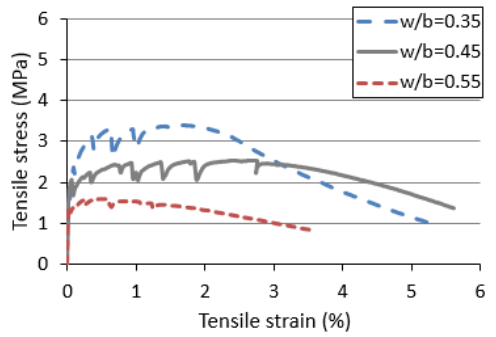

(a)

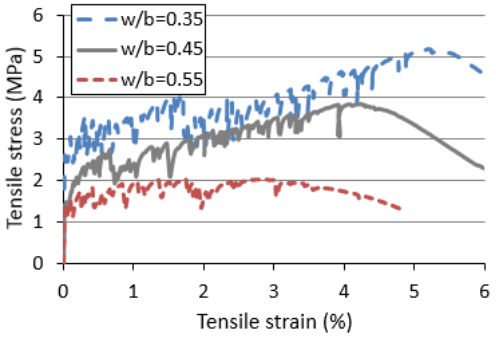

(b)

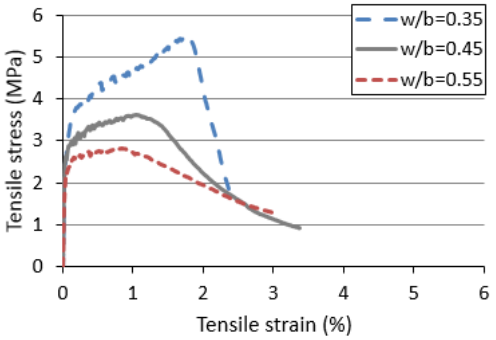

(c)

Fig. 2 Representative tensile stress and strain curves: (a) PP fiber series; (b) PE fiber series; and (c) PBO fiber series

specimen using an electronic universal testing machine. The tensile load was measured by a load cell, and the deformation of the specimen was measured by two linear variable differential transducers. The tensile stress and strain were calculated from the load and deformation, respectively. The geometry of the specimen for the tension test and the test setup are shown in Fig. 1. The crack pattern of each mixture was investigated by measuring the number of cracks from the unloaded specimen after the uniaxial tension test. The number of cracks in each case was counted manually within a gauge length of 80 mm on both sides of each specimen. The crack spacing was calculated by dividing the gauge length (80 mm) by the number of cracks. The crack width was calculated indirectly by dividing the total amount of deformation by the number of cracks within a gauge length of 80 mm. It was assumed that all deformations occurring at cracks and were identical to the sum of the crack openings because the deformation of the matrix is much smaller than a crack opening (Kang *et al.* 2016).

Table 4 Compressive strength of each mixture

Type of fiber	Water-to-binder ratio		
	0.35	0.45	0.55
PP	36.8±1.6	20.2±0.5	8.8±0.1
PE	39.8±0.3	24.0±1.1	11.1±0.3
PBO	40.1±0.4	19.7±0.6	11.8±0.3

3. Results and discussion

3.1 Compressive strength

As expected, the compressive strength increased with a decrease in the water-to-binder ratio. The maximum difference in the compressive strength of the composite with the same water-to-binder ratio ranged from 8.1% to 25.2%. Although the PBO fiber had the highest tensile strength among three types of fibers, it was not significantly effective with regard to its ability to increase the compressive strength of the composite compared to the PP and PE fibers.

3.2 Uniaxial tensile behavior

Fig. 2 shows the representative tensile stress and strain curves of each mixture according to the types of fibers used. The tensile stress and strain curve closest to the average tensile strength and tensile strain capacity of each mixture was selected as a representative tensile stress and strain curve among six curves of each mixture. All mixtures showed tensile strain-hardening behavior under a tensile load with multiple cracks, which is not observed in normal concrete and fiber-reinforced concrete. There were higher stress drops in the PP fiber series and PE fibers series composites than in the PBO fiber series composites. This is attributed to the low chemical bond between the fiber and the matrix of the PP series and PE fibers series composites. Fiber bridging curve of a composite reinforced by hydrophobic fiber starts at low stress level and in a zero crack-opening state, mainly due to a frictional bond between the fiber and the matrix with a low chemical bond between these components. Therefore, there is generally observed a higher stress drop in a hydrophobic fiber-reinforced composite than in a hydrophilic fiber-reinforced composite when a crack occurs. These test results indicated indirectly that the PBO fiber has the less hydrophobic surface property than the PP and PE fibers.

Fig. 3 shows the representative tensile stress and strain curves of each mixture according to the water-to-binder ratio. For all water-to-binder ratios, the PE fiber series composites had higher tensile strength and tensile strain capacity levels than the PP fiber series composites. This was mainly due to the low tensile strength of the PP fiber, compared to PE fiber. Although the tensile strength of the PBO fiber was 91% higher than that of the PE fiber, the tensile strain capacity of the PBO fiber series composites was lower than that of the PE fiber series composites. This was likely due to the excessive bonding between the PBO fiber and the matrix, as indirectly proved by the fact that there was only a slight stress drop in the PBO fiber series

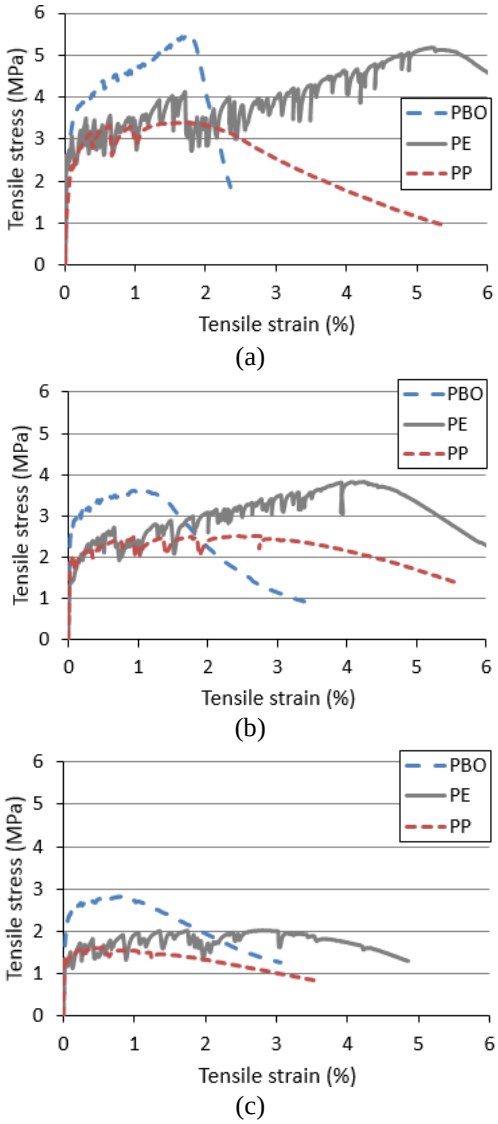

Fig. 3 Representative tensile stress and strain curves according to the water-binder ratios of (a) 0.35, (b) 0.45, and (c) 0.55

composites.

Table 5 lists the first-cracking strength of each mixture. With regard to the first-cracking strength, the first-cracking strength increased with a decrease in the water-to-binder ratio. Although the different types of fibers has not influenced the compressive strength of the composites, the type of fiber has effects on the first-cracking strength. The first-cracking strength of the PBO fiber series composites was on average 62.3% and 77.6% higher than those of the PP fiber series and PE fiber series composites, respectively. This may be attributed to the strong bond between the PBO fiber and the matrix.

Table 6 lists the tensile strength of each mixture. The tensile strength increased as the water-to-binder ratio decreased and as the tensile strength of the fiber increased. This is attributed to the fact that the interfacial bond between the fiber and the matrix increased with a decrease in the water-to-binder ratio and the number of ruptured fibers on the crack plane decreased with an increase in the

Table 5 First-cracking strength (unit: MPa)

Type of fiber	Water-to-binder ratio		
	0.35	0.45	0.55
PP	2.91±0.39	1.88±0.29	1.45±0.17
PE	2.12±0.34	1.95±0.35	1.43±0.21
PBO	3.81±0.11	3.22±0.44	2.68±0.23

Table 6 Tensile strength (unit: MPa)

Type of fiber	Water-to-binder ratio		
	0.35	0.45	0.55
PP	3.24±0.26	2.58±0.25	1.53±0.15
PE	4.82±0.41	3.71±0.43	2.06±0.16
PBO	5.75±0.25	3.71±0.44	3.19±0.38

Table 7 Tensile strain capacity (unit: %)

Type of fiber	Water-to-binder ratio		
	0.35	0.45	0.55
PP	1.94±1.01	3.00±0.35	0.93±0.56
PE	4.93±0.45	3.94±0.80	3.67±0.70
PBO	1.86±0.27	0.99±0.14	1.04±0.24

tensile strength of the fiber. The tensile strength of fiber-reinforced concrete is not a matrix property but instead depends on the fiber bridging capacity at the crack plane, and it is identical to the minimum fiber bridging stress in the composite. Therefore it is necessary to tailor the properties of the fiber and the interfacial properties between the fiber and the matrix to improve the tensile strength of composite.

Table 7 lists the tensile strain capacity of each mixture. Overall, the PE fiber series composites had the highest tensile strain capacity among all types of fibers. Although the PBO fiber had higher tensile strength by 91% compared to the PE fiber, the average tensile strain capacity of the PBO fiber series composites was 70% lower on average than that of the PE fiber series composites. The lower tensile strain capacity of the PBO fiber series composites compared to the PE fiber series composites may have arisen mainly because of the strong bond between the PBO fiber and the matrix, which can induce a high fiber bridging capacity. However, a strong bond can decrease the complementary energy in the fiber bridging curve, which induces less steady-state cracking behavior (Li *et al*. 2001, Kanda and Li 2006). Li *et al.* (2001) improved the tensile strain capacity of a PVA fiber-reinforced cementitious composite by proper oil-coating of the PVA fiber, which decreased the tendency of hydrophilicity of the fiber and the chemical bond between the PVA fiber and the matrix, proving the fiber-matrix tailoring concept. From earlier work (Li *et al*. 2001) and the test results, we concluded that a higher tensile stain capacity of a PBO fiber-reinforced composite is attainable by tailoring the surface properties of the PBO fiber. Another reason for the lower tensile strain capacity of the PBO fiber series composites was that the elastic modulus of the PBO fiber was higher than that of the PE fiber. In fact, the elastic modulus of the PBO fiber was 1.61 times higher than that of the PE fiber. The elastic

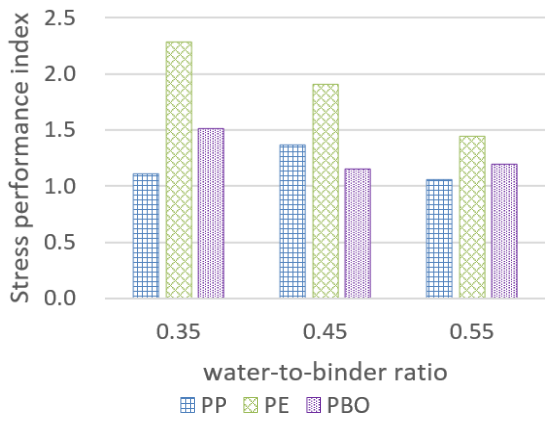

Fig. 4 Stress performance index (ratio of the tensile strength to the first-cracking strength)

deformation of the fiber depends on the elastic modulus under the same amount of stress. Therefore, the elastic deformation of the PBO fiber at the crack plane was 0.62 times less than that of the PE fiber. Low elastic deformation of the fiber at the crack plane induced a low crack width, which resulted in low permeability and improved durability. However, it induced a low tensile strain capacity.

The tensile strain capacity of the PE fiber series and PBO fiber series composites increased with a decrease in the water-to-binder ratio. On the other hand, the maximum tensile strain capacity of the PP fiber series composites was observed when the water-to-binder ratio was 0.45. The PP-0.45 mixture had a higher tensile strain capacity than the PP-0.55 mixture and the PP-0.35 mixture, as seen in Table 7. Although the PBO fiber had a higher tensile strength and a higher aspect ratio than the PE fiber, the PBO fiber series composites had a lower tensile strain capacity than the PE fiber series composites. These test results confirmed that a high tensile strain capacity is attainable by adopting an appropriate matrix strength level when a type of fiber with low tensile strength is used as a reinforcing fiber and when the interfacial property is the main factor influencing the tensile strain capacity of the composite.

Kanda and Li proposed what can be referred to as a two-performance index, i.e., a stress performance index and an energy performance index, to express the potential of the strain-hardening behavior with multiple saturated cracks (Kanda and Li 2006). The stress performance index is defined as the ratio of the maximum fiber bridging stress to the cracking strength of the composite. The energy performance index is defined as the ratio of the complementary energy that can be calculated from the fiber bridging curve to the fracture toughness of the matrix. A higher tensile strain capacity is achievable with higher performance indices. It is necessary to undertake a matrix fracture toughness test and a single fiber pullout test to evaluate the performance index on the micromechanical scale. The stress performance index can be calculated indirectly from the ratio of the tensile strength to the first-cracking strength.

Fig. 4 shows the stress performance index for each mixture. All mixtures had a stress performance index exceeding 1, indicating that all the mixtures satisfied the minimum requirement of the stress performance index for the strain-hardening behavior with multiple saturated cracks. The PE fiber series composites with a higher tensile strain capacity exhibited a higher stress performance index than the PP and the PBO fiber series composites. Overall, the composites with a higher stress performance index demonstrated higher tensile strain capacities. These test results experimentally confirmed that the stress performance index is strongly correlated with the tensile strain capacity.

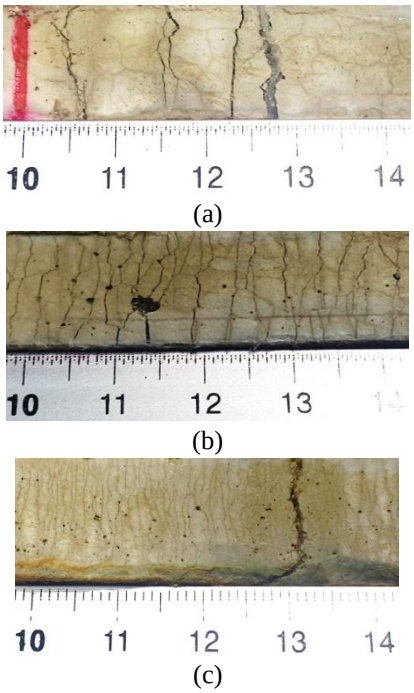

Fig. 5 Crack patterns (unit of numbers: cm): (a) PP-0.35, (b) PE-0.35, and (c) PBO-0.35

Fig. 5 shows the crack patterns of the PP, PE, and PBO fiber-reinforced composites with a water-to-binder ratio of 0.35. All specimens had multiple micro-cracks and one large crack at which arises the failure plane and the minimum fiber bridging capacity. Although all three specimens showed multiple cracks, the crack patterns were quite different. The PP-0.35 mixture had a smaller number of cracks with greater crack widths and spacing distances than the PE-0.35 mixture. On the other hand, the PBO-0.35 mixture had a greater number of cracks with smaller crack widths and spacing distances than the PE-0.35 mixture.

Fig. 6 shows the number of cracks for each mixture. The number of cracks in the PBO-0.45 and PBO-0.55 mixtures could not be counted because the crack width of those specimens were too narrow. The average number of cracks in the PE fiber series composites with identical water-to-binder ratios was 5.9 times higher than that of the PP fiber series composites, and the average number of cracks of the PBO-0.35 mixture was 1.9 times higher than that of the PE-0.35 mixture. It can be assumed that all deformations occur at cracks because the deformation of the matrix is much smaller than the crack opening. Thus, the tensile strain capacity of a composite depends on the number of cracks and the crack width. Therefore, the higher the number of

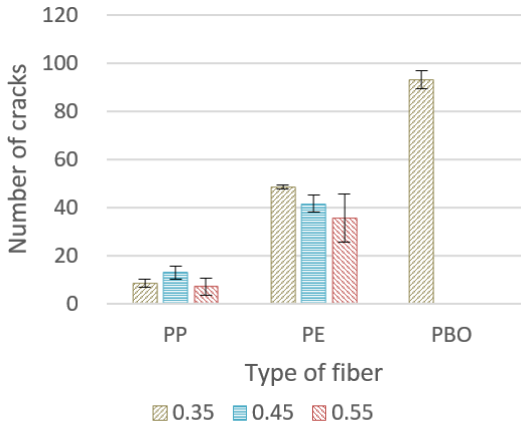

Fig. 6 Number of cracks within a gauge length of 80 mm

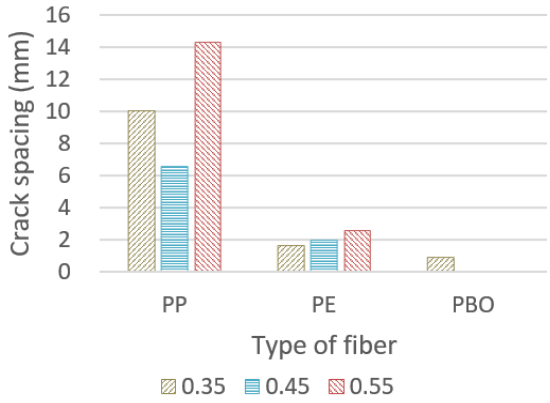

Fig. 7 Crack spacing

cracks and the wider the crack widths (up to critical crack width, in most cases less than 100 μm), the higher the potential of the tensile strain capacity. It was observed that the number of cracks in the PP-0.45 mixture, which had the highest tensile strain capacity among the PP fiber series composites, was higher than those of PP-35 and PP-55 mixtures, and the number of cracks in the PE fiber series composites increased with an increase in the tensile strain capacity.

Fig. 7 shows the crack spacing of each mixture. The PE fiber series composites and PBO-0.35 mixture showed saturated crack patterns. The average crack spacing of the PE fiber series composites was 2.1 mm and the average crack spacing of PBO-0.35 mixture was 0.86 mm, which was 48 % lower than that of the PE-0.35 mixture. On the other hand, the average crack spacing of the PP fiber series composites was 10.3 mm, which was 5.0 times higher than that of the PE fiber series composites.

Fig. 8 shows the average crack width of each mixture. It was observed that crack width of the PP fiber series composites was influenced more by the water-to-binder ratio compared with the PE fiber series composites. The average crack width of the PE fiber series composites was 85.4 μm. The average crack width of the PP fiber series composites was 144.6 μm, which was 1.7 times higher than that of the PE fiber series composites. The average crack width of the PBO-0.35 mixture was 17.2 μm, which was 80% lower than that of the PE-0.35 mixture. As described

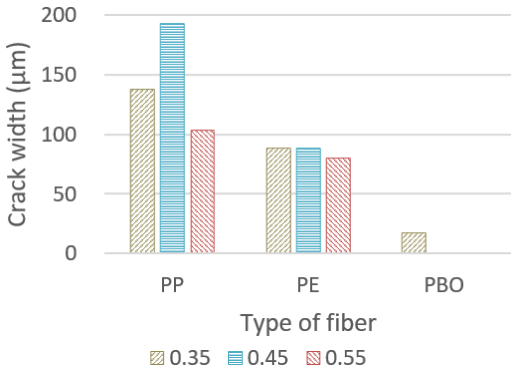

Fig. 8 Crack width

above, a small crack width could result in lower permeability and therefore increase the durability performance. However, it also influenced the tensile strain capacity of the composite, which should therefore be optimized according to the target performance in terms of durability and ductility.

4. Conclusions

This study experimentally investigated the tensile behavior of alkali-activated slag-based cementless composites reinforced by synthetic fibers. We performed a series of experimental tests, including a compressive strength test and a uniaxial tension test. From the experimental test results, it was exhibited that the PE fiber series composites had the highest tensile strain capacities among the three types of fiber series composites, a tight crack width of below 100 μm, and saturated crack patterns. On the other hand, the PP fiber series composites demonstrated lower tensile behavior in terms of the tensile strength and tensile strain capacity as compared to the PE fiber series and the PBO fiber series composites. The PP fiber series composites also had wider crack widths than the PE fiber series and PBO fiber series composites. Although the PBO fiber had higher tensile strength by 91% than the PE fiber, the tensile strength of the PBO fiber series composites had only higher tensile strength by 25% on average than the PE fiber series composites, and the PBO fiber series composites had a lower tensile strain capacity by 70% on average than the PE fiber series composites. We attributed this to the excessively strong bond between the PBO fiber and the matrix and to the high elastic modulus of the fiber. However, the fact that the number of cracks in the PBO-0.35 mixture was 92% higher than that in the PE-0.35 mixture demonstrated that the potential to improve the tensile strain capacity and tensile strength of the PBO fiber series composites is high when tailoring the interfacial properties between the PBO fiber and the matrix.

Acknowledgments

This research was supported by Basic Science Research Program through the National Research Foundation of

Korea (NRF) funded by the Ministry of Science and ICT (NRF-2016R1A1A1A05005208 and No. 2015R1A5A1037548).

References

ASTM (2007), Standard Test Method for Compressive Strength of Hydraulic Cement Mortars (Using 2-in. or (50-mm) cube specimens), American Society for Testing and Materials, ASTM International West Conshohocken, PA.

Cho, C.G., Lim, H.J., Lee, B.Y. and Choi, Y. (2015), "Experiments and performances of strain-hardening fiber low cementitious composites", *Adv. Mech. Eng.*, **7**(6), 1-7.

Choi, J.I., Lee, B.Y., Ranade, R., Li, V.C. and Lee, Y. (2016), "Ultra-high-ductile behavior of a polyethylene fiber-reinforced alkali-activated slag-based composite", *Cem. Concr. Compos.*, **70**, 153-158.

Choi, J.I., Song, K.I., Song, J.K. and Lee, B.Y. (2016), "Composite properties of high-strength polyethylene fiber-reinforced cement and cementless composites", *Compos. Struct.*, **138**, 116-121.

Choi, S.J., Choi, J.I., Song, J.K. and Lee, B.Y. (2015), "Rheological and mechanical properties of fiber-reinforced alkali-activated composite", *Constr. Build. Mater.*, **96**, 112-118.

Felekoglu, B. and Keskinates, M. (2016), "Multiple cracking analysis of HTPP-ECC by digital image correlation method", *Comput. Concrete*, **17**(6), 831-848.

Felekoglu, B., Tosun-Felekoglu, K., Ranade, R., Zhang, Q. and Li, V.C. (2014), "Influence of matrix flowability, fiber mixing procedure, and curing conditions on the mechanical performance of HTPP-ECC", *Compos. Part B Eng.*, **60**, 359-370.

Huang, J. and Huang, P. (2011), "Three-dimensional numerical simulation and cracking analysis of fiber-reinforced cement-based composites", *Comput. Concrete*, **8**(3), 327-341.

JSCE (2008), Recommendations for Design and Construction of High Performance Fiber Reinforced Cement Composites with Multiple Fine Cracks (HPFRCC), Japan Society of Civil Engineers, Japan.

Kanda, T. and Li, V.C. (1998), "Interface property and apparent strength of high-strength hydrophilic fiber in cement matrix", *J. Mater. Civil. Eng.*, ASCE, **10**(1), 5-13.

Kanda, T. and Li, V.C. (2006), "Practical design criteria for saturated pseudo strain hardening behavior in ECC", *J. Adv. Concr. Technol.*, **4**(1), 59-72.

Kang, S.T., Choi, J.I., Koh, K.T., Lee, K.S. and Lee, B.Y. (2016), "Hybrid effects of steel fiber and microfiber on the tensile behavior of ultra-high performance concrete", *Compos. Struct.*, **145**, 37-42.

Kang, S.T., Lee, K.S., Choi, J.I., Lee, Y., Felekoğlu, B. and Lee, B.Y. (2016), "Control of tensile behavior of ultra-high performance concrete through artificial flaws and fiber hybridization", *Int. J. Concrete Struct. Mater.*, **10**(3), 33-41.

Lee, B.Y., Cho, C.G., Lim, H.J., Song, J.K., Yang, K.H. and Li, V.C. (2012), "Strain hardening fiber reinforced alkali-activated mortar-A feasibility study", *Constr. Build. Mater.*, **37**, 15-20.

Lee, B.Y., Kim, J.K. and Kim, Y.Y. (2010), "Prediction of ECC tensile stress-strain curves based on modified fiber bridging relations considering fiber distribution characteristics", *Comput. Concrete*, **7**(5), 455-468.

Lee, B.Y., Lee, Y., Kim, J.K. and Kim, Y.Y. (2010), "Micromechanics-based fiber-bridging analysis of strain-hardening cementitious composite accounting for fiber distribution", *CMES-Comp. Model. Eng. Sci. CMES-Comp. Model. Eng. Sci.*, **61**(2), 111-132.

Li, M. and Li, V.C. (2013), "Rheology, fiber dispersion, and robust properties of engineered cementitious composites", *Mater. Struct.*, **46**(3), 405-420.

Li, M., Luu, H.C., Wu, C., Mo, Y. and Hsu, T.T. (2014), "Seismic performance of reinforced engineered cementitious composite shear walls", *Earthq. Struct.*, **7**(5), 691-704.

Li, V.C. (2012), "Tailoring ECC for special attributes: A review", *Int. J. Concrete Struct. Mater.*, **6**(3), 135-144.

Li, V.C., Wang, S. and Wu, C. (2001), "Tensile strain-hardening behavior of polyvinyl alcohol engineered cementitious composite (PVA-ECC)", *ACI Mater. J.*, **98**(6), 483-492.

Maalej, M. and Li, V.C. (1994), "Flexural/tensile-strength ratio in engineered cementitious composites", *J. Mater. Civil. Eng.*, ASCE, **6**(4), 513-528.

Nematollahi, B., Sanjayan, J. and Ahmed Shaikh, F.U. (2015), "Tensile strain hardening behavior of PVA fiber-reinforced engineered geopolymer composite", *J. Mater. Civil. Eng.*, ASCE, 04015001.

Nematollahi, B., Sanjayan, J. and Shaikh, F.U.A. (2015), "Strain hardening behavior of engineered geopolymer composites: effects of the activator combination", *J. Aust. Ceram. Soc.*, **51**(1), 54-60.

Ohno, M. and Li, V.C. (2014), "A feasibility study of strain hardening fiber reinforced fly ash-based geopolymer composites", *Constr. Build. Mater.*, **57**, 163-168.

Ranade, R., Li, V.C., Stults, M.D., Heard, W.F. and Rushing, T.S. (2013), "Composite properties of high-strength, high-ductility concrete", *ACI Mater. J.*, **110**(4), 413-422.

Tosun-Felekoğlu, K., Gödek, E., Keskinateş, M. and Felekoğlu, B. (2017), "Utilization and selection of proper fly ash in cost effective green HTPP-ECC design", *J. Clean Prod.*, **149**, 557-568.

Yang, E.H., Wang, S., Yang, Y. and Li, V.C. (2008), "Fiber-bridging constitutive law of engineered cementitious composites", *J. Adv. Concrete Technol.*, **6**(1), 181-193.

HK